Letter

Accelerating Neurite Growth and Directing Neuronal Connections Constrained by 3D Porous Microtubes

Shengying Fan, Lei Qi, Jiawen Li,* Shunli Liu, Rui Li, Tongzhou Zhan, Xiaowei Li, Dong Wu, Pakming Lau,* Bensheng Qiu, Guoqiang Bi, and Weiping Ding*

Read Online

ACCESS | Metrics & More | Article Recommendations | Supporting Information

ABSTRACT: Investigation of neural growth and connection is crucial in the field of neural tissue engineering. Here, using a femtosecond laser direct writing (fs-DLW) technique, we propose a directionally aligned porous microtube array as a culture system for accelerating the growth of neurons and directing the connection of neurites. These microtubes exhibited an unprecedented guidance effect toward the outgrowth of primary embryonic rat hippocampal neurons, with a wrap resembling the myelin sheaths of neurons. The speed of neurite growth inside these microtubes was significantly faster than that outside these microtubes. We also achieved selective/directing connection of neural networks inside the magnetic microtubes via precise microtube delivery to a gap between two neural clusters. This work not only proposes a powerful microtube platform for accelerated growth of neurons but also offers a new idea for constructing biological neural circuits by arranging the size, location, and pattern of microtubes.

KEYWORDS: *femtosecond laser writing, porous microtubes, coaxial constraints, neurite growth, neuronal connections*
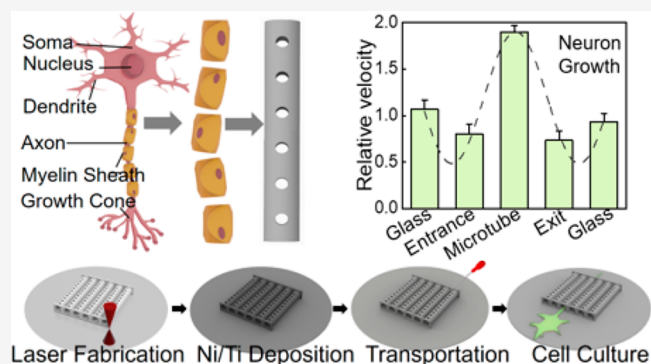
Investigation of neural growth and connection is crucial in the field of tissue engineering.[1,2] By accelerating the growth of neurons and directing the connection of neurites *in vitro*, rapidly reconstructed neural circuits can be effectively used to study neural repair, neural therapeutics, and even neurodegenerative disease and brain cognition mechanisms.[3–5] To engineer the growth and connectivity of neurons *in vitro*, neurite chemical guidance has been proposed. Kam et al. demonstrated that polylysine-conjugated laminin, a highly selective protein, can effectively provide chemical guidance for axonal growth.[6] Meanwhile, a variety of neurite physical guidance approaches have also been proposed.[7–10] For example, Kim et al. reported a neuron-loaded microgroove for directing the growth direction of neurites and selective connection of neural networks.[11] However, *in vivo* conditions are three-dimensional (3D) by nature, and many axons are ensheathed in glial cell membranes (myelin).[12] The above cell culture cases were all on open surfaces and could not fully show normal cell growth, proliferation, and differentiation functions.

Recently, tremendous efforts have also been made to develop nerve conduits with polymers and graphene oxide (GO) to guide neural growth.[13–18] These studies show that nerve guidance conduits (NGCs) can offer a potentially interesting platform for promoting the regeneration of neurites and constructing biological neural networks. However, the size

of the reported NGCs is far larger than the diameter of the neurites (usually hundreds of microns or even millimeters), and they hardly guide the growth of axons and dendrites of a single neuron. In this instance, Froeter et al. presented a neuron cell culturing platform consisting of arrays of ordered microtubes that can guide accelerated growth of neuronal axons.[19] Cangellaris et al. proposed a substrate constructed of arrays of strain-induced self-rolled-up membrane 3D architectures to guide hippocampal neurons to form neural circuits.[20] However, the above-mentioned microtube preparation adopts the traditional strain-induced self-rolled-up method, which has a complicated preparation process and poor 3D forming ability. Femtosecond laser direct writing (fs-DLW) technology has the advantages of simplicity, true 3D, high resolution, and flexibility in micro/nanofabrication and has already been adopted by many pioneers to build simple scaffolds to support cell growth[21] or to develop controlled 3D cellular networks.[22] However, it has not been used to fabricate
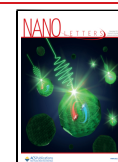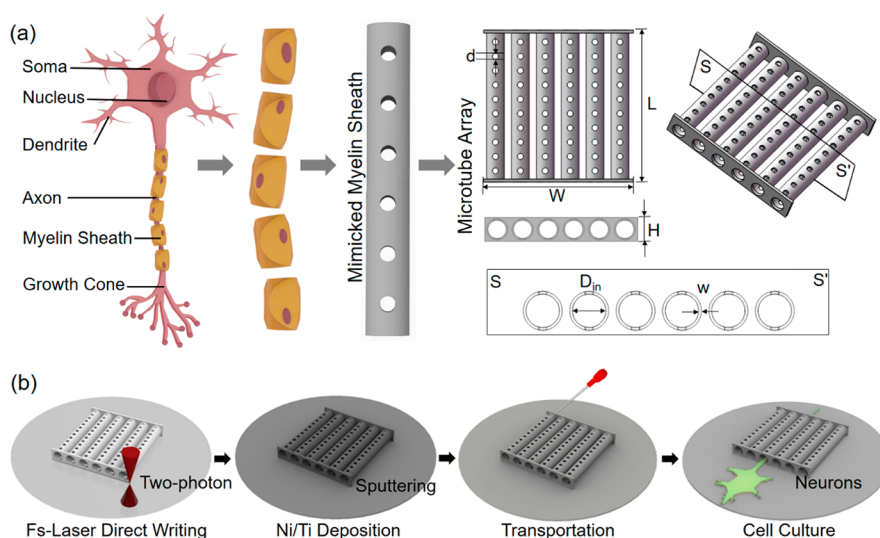
Figure 1. Design and fabrication of porous microtubes for accelerated growth of neurites and directed neuronal connections. (a) A porous microtube mimicking the axonal myelin sheath and computer-aided design of microtubes. (b) Schematic fabrication process of microtubes, femtosecond direct laser writing (fs-DLW), and deposition of nickel (Ni, for magnetic properties)/titanium (Ti, for biocompatibility) on microtubes.

microtube structures for guided neurite growth and connection.

In this study, we fabricated porous microtubes using an fs-DLW method and achieved accelerating growth of neurites and guided directing connection of neurons. We exploited the growth of neuronal neurites in differently sized microtubes, evaluated the speed of neurite growth/extension at different locations of microtubes, and finally uncovered the relationship between neurite growth velocity and porous microtube parameters, including inner diameter, wall thickness, and tube length. The size of NGCs is close to the myelin sheath, accelerating the speed of nerve regeneration and shortening the recovery time of nerve injury. In addition, to demonstrate the ability of the microtubes to selectively connect nerve clusters to form specific neural networks, the movement of magnetic-coated microtubes to a designated position is controlled by a permanent magnet to guide the directional growth of axons and dendrites of neurons. The controllable array direction of NGCs ensures the expected directional conduction in a specific neural circuit, which is an indispensable process for the development of the nervous system.

Design and fabrication of porous microtubes for accelerated growth of neurites and directed neuronal connections. To provide 3D scaffolds that guide and confine individual axons or dendrites, we are inspired by axonal myelin sheaths to design microtubes (Figure 1a). The size of microtubes is precisely controlled within a range slightly larger than typical axons (2–3 μm) in diameter because small microtubes hardly ensure inner-tubular growth of neurites, while oversized microtubes tend to include multiple axons or even neural somas.[19] Here, we design and fabricate microtubes with different sizes to guide the accelerated growth and directed connection of neurites. Figures 1b and S1 show the porous microtubes we fabricated with fs-DLW (the laser scanning step was 200 nm in all directions, the exposure time was 1000 μs, and the exposure power was 10 mW). To endow the microtubes with magnetic properties and biocompatibility, 100 nm Ni and 40 nm Ti thin films were deposited on the fabricated microtubes (the

deposited elements were characterized in Figure S2; the two films tightly stuck to the microtubes even after being immersed in the medium for 13 days). Thus, magnetic microtubes can be moved to specific locations with a permanent magnet (Figure S3; Videos S1, S2, and S3).

For the microtubes, there are walls with a height of 10 μm at both ends to prevent neurites from passing above the microtubes or the gaps between the microtubes as much as possible. Here, we design and fabricate microtubes with inner diameters of 4, 6, and 8 μm, wall thicknesses of 0.5, 0.75, and 1 μm, and lengths of 85, 120, and 155 μm (Figure S4). In addition, pores with a diameter of 1 μm and a spacing of 4 μm are designed on the walls of the microtubes to facilitate the transport of substances for the growth of neurites.[23,24] Compared with microfluidic chambers, the microtube we designed is a true 3D round one, the microtube is separable from the substrate and movable after magnetic sputtering, and the wall of the microtube is porous for nutrition exchange.

Accelerated growth of neurites by microtubes: effect of microtube inner diameter. To obtain the microtube size that is most effective for neural guidance and growth, the effects of microtube inner diameter, wall thickness, and length on neurite growth are systematically studied. Dynamic neural growth within the microtubes is adopted using live-cell recording. Figure 2a shows a typical neurite outgrowth in a porous microtube array of live-cell recordings (also see Video S4; the time and location of the neurites in the microtubes were determined according to the corresponding videos). To demonstrate the general guidance effects of the microtube structure similar to the myelin sheath (Figure 2b), the average growth velocities of hippocampal neurites are schematically studied on the planar glass substrate (location 1) near the microtube entrance, at the microtube entrance (location 2), in the microtube (location 3), at the microtube exit (location 4), and on the planar glass substrate (location 5) near the microtube exit.

A growing axon has a highly mobile structure at its front end, called a growth cone, which detects signals from the extracellular environment to guide its growth direction. The
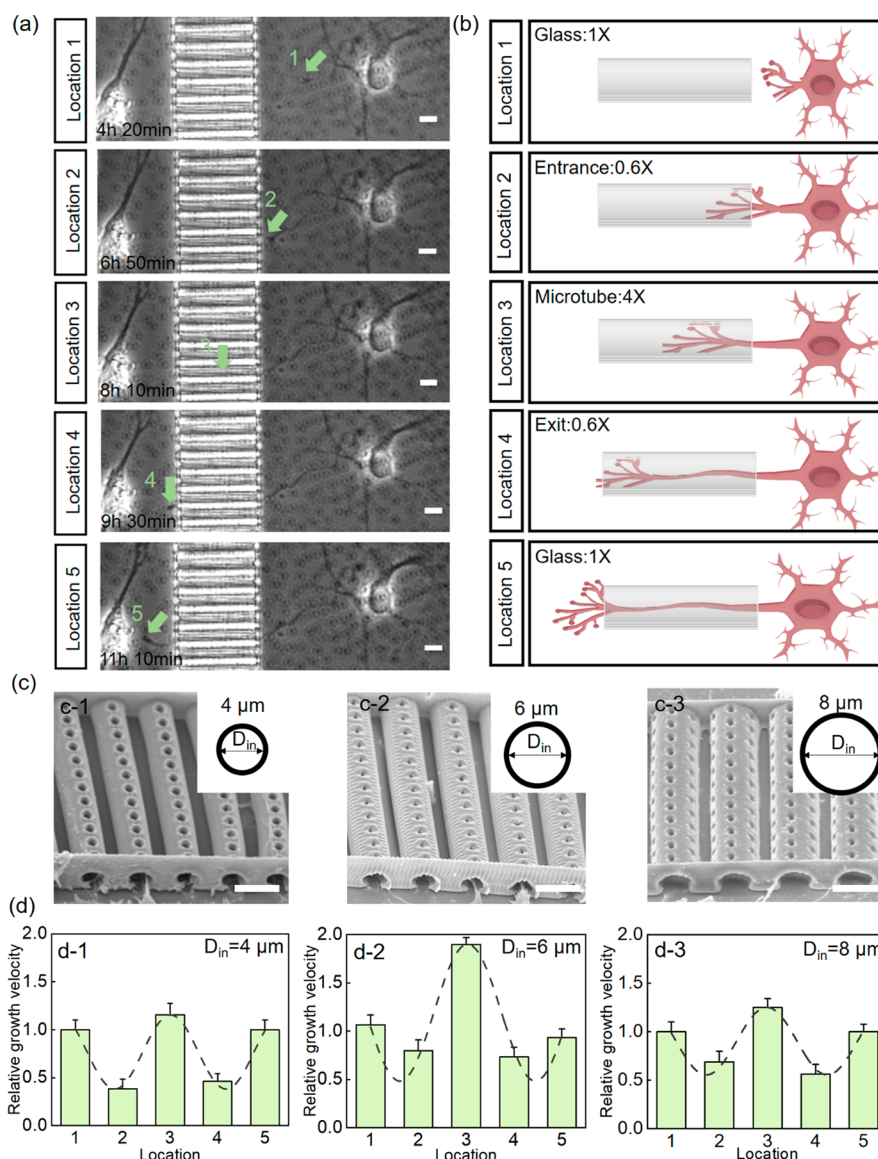
Figure 2. Accelerated growth of neurites by microtubes: effect of microtube inner diameter. (a) Time-lapse phase contrast images of a living hippocampal neuron showing neurite pathfinding through a microtube. Each frame, from top to bottom, represents the growth cone location (green arrows) at time points (from top to bottom): 4 h 20 min on a planar glass substrate; 6 h 50 min at a microtube inlet; 8 h 10 min inside a microtube; 9 h 30 min at a microtube outlet; 11 h 10 min back on a planar glass substrate. Original Video S4 of the living cell recording is included in the Supporting Information. (b) Schematic of the neurite growth velocity of a single neuron in the presence of a microtube: on the planar glass substrate (1) near the microtube entrance, at the microtube entrance (2), in the microtube (3), at the microtube exit (4), and on the planar glass substrate (5) near the microtube exit. (c) SEM images show that hippocampal neurites are cultured at 6 days *in vitro* (DIV) in microtubes with inner diameters of 4 μm (c-1), 6 μm (c-2), and 8 μm (c-3). (d) Relative growth velocity (μm/min) is calculated at 25 μm intervals from the living cell recording and the velocities of five locations (the gray dotted line is fitted by the sine function of Origin's nonlinear curve fitting method). (*n* = 15 samples and three separate cultures each.) The Origin software package was used for the statistical analysis. Here, the microtubes have a wall thickness of 0.75 μm and a length of 50 μm. Scale = 10 μm.

growth cones activate some receptors, such as Yes-associated protein (YAP),[25] focal adhesion kinase (FAK),[26] and integrin-linked kinase (ILK)[27] to recognize guiding factors and convert signals into chemotaxis reactions. It is generally believed that when the growth cone detects the targeting factor, the receptor will activate a variety of signaling molecules in the growth cones and ultimately affect the growth velocity of the neurons (Figure S5).[28] At 4 h 20 min, the axonal growth cone explored the growth paths on the flat glass substrate (Figure 2a, location 1). At 6 h 50 min and 8 h 10 min, the growth cone contacted the entrance and subsequently extended into the microtubes (locations 2 and 3). At 9 h 30 min and 11 h 10 min, the growth

cone arrived at the exit of the microtubes and then grew back onto the flat substrates (locations 4 and 5). Here, the rates of the extension/growth acceleration of neurites in the micro-tubes with 4, 6, and 8 μm were approximately 2.78, 11.11, and 3.56 μm/h^2, respectively. Axonal outgrowth and pathfinding are mainly controlled by dynamic microtube/F-actin inter-actions and corresponding filopodia dynamics in response to substrate cues.[29]

Hippocampal neurites were cultured for 3 days *in vitro* (DIV) in microtubes with different inner diameters under a wall thickness of 0.75 μm and a length of 50 μm (Figures 2c and S6). The images show that most of the neurites grow from
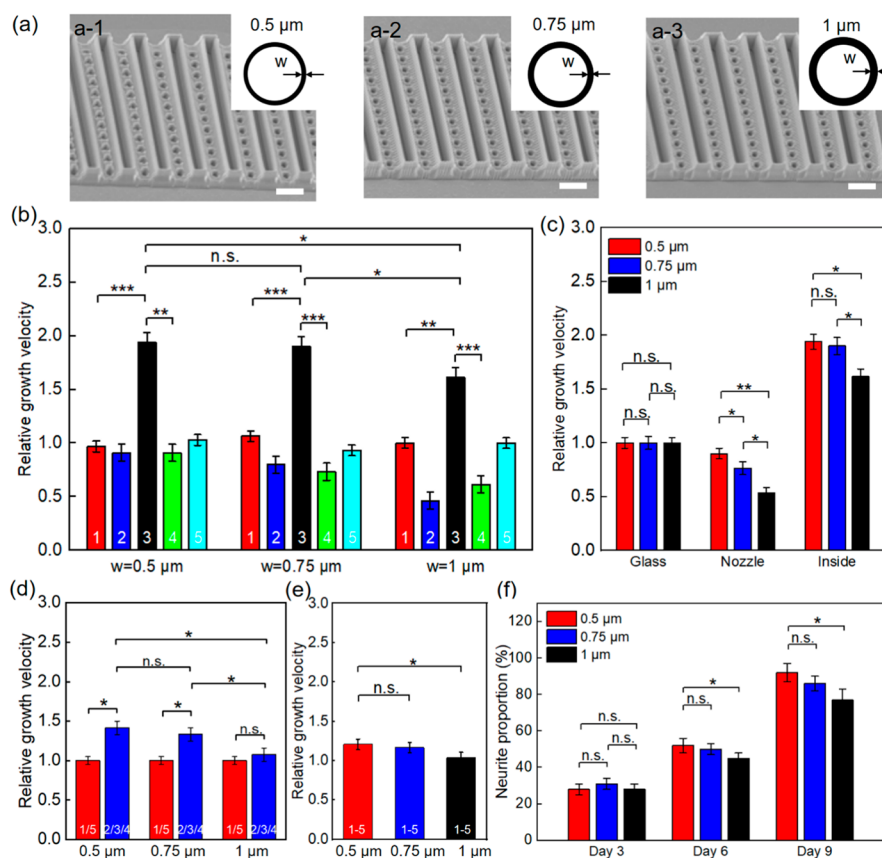
Figure 3. Accelerated growth of neurites by microtubes: effect of microtube wall thickness. (a) SEM images show microtubes with different wall thicknesses; the wall thicknesses are 0.5, 0.75, and 1 μm. (b) Relative growth velocity (μm/min) is calculated at five locations of microtubes with different wall thicknesses. (c) Relative growth velocity is calculated at glass and microtube nozzles and inside microtubes. (d) Relative speed of neurite growth within microtubes with different wall thicknesses at different locations was calculated. Position 1/5 denotes the average velocity of neurites on glass substrates on both sides of the microtubes. Position 2/3/4 denotes the average velocity of neurites at the microtube entrance, exit, and inside the microtubes. (e) Relative speed of neurite growth within microtubes with different wall thicknesses was calculated. Positions 1−5 denote the total average velocity of neurites on glass substrates and microtubes. (f) The proportion of neurite growth on microtubes with different wall thicknesses at 3, 6, and 9 DIV. (n = 15 samples and three separate cultures each). The Origin software package was used for the statistical analysis, followed by one-way ANOVA (*$p < 0.05$, **$p < 0.01$, ***$p < 0.001$, n.s., no significance). Here, the microtubes have an inner diameter of 6 μm and a length of 50 μm. Scale = 5 μm.

the microtube inlets into the microtubes. When the inner diameters are 4, 6, and 8 μm, in different locations of microtubes, the growth velocity of neurons tends to be consistent (Figure 2d, gray dotted curves). The speed of neurite growth in the microtubes was significantly higher than that at the microtube inlets and outlets and on the glass substrates (the extension of neurites on the glass substrate in culture dish, as shown in Figure S7). The major factor for the rapid growth of neurites in microtubes is the complete radial confinement of axons and dendrites provided by an appropriate tubular scaffold.[30,31] When the branch is limited by spatial confinement, radially constrained actin polymerization facilitates axial extension of neurites and thus speeds up the growth of neurites. At the entrance and exit of the microtubes, because the microtubes have a thick wall, the neurites need pathfinding to climb and grow, resulting in a slower growth velocity. In addition, we also found that the average speed of neurite growth in the microtubes with inner diameters of 6 μm was fastest. The reason is that in the microtubes with a smaller inner diameter, the neurites have longer pathfinding times at the entrance of the microtubes, while in the microtubes with a larger inner diameter, the

tubular scaffolds provide less radial constraint on axons and dendrites.

To further confirm that neurites are guided by microtubes to grow directionally, hippocampal neurons were cultured on poly-L-lysine-coated microtubes with different inner diameters and then labeled with two immunofluorescence markers, tau and MAP2, at 3, 6, and 9 DIV (Figure S8). Surprisingly, neural circuits can be formed between neurons in different microtubes (synapse formation can also be observed in the microtubes, as shown in Figures S9 and S10). In addition, with increasing culture time, the number of neurites in the microtubes increased. After 9 DIV, the proportion of microtubes containing neurites ([the number of microtubes with neurites/the total number of microtubes] × 100%) reached more than 80% (Figure S11). Furthermore, we also achieve a more interesting scenario, in which only one axon or dendrite is allowed to grow in a microtube with an inner diameter of 2 μm for 3 days (Figure S12 and Video S5).

Accelerated growth of neurites by microtubes: effect of microtube wall thickness. Benefiting from the high-resolution advantage of femtosecond laser direct writing, we designed and fabricated microtubes with different wall thicknesses (the inner diameter of microtubes is 6 μm based on the above-mentioned
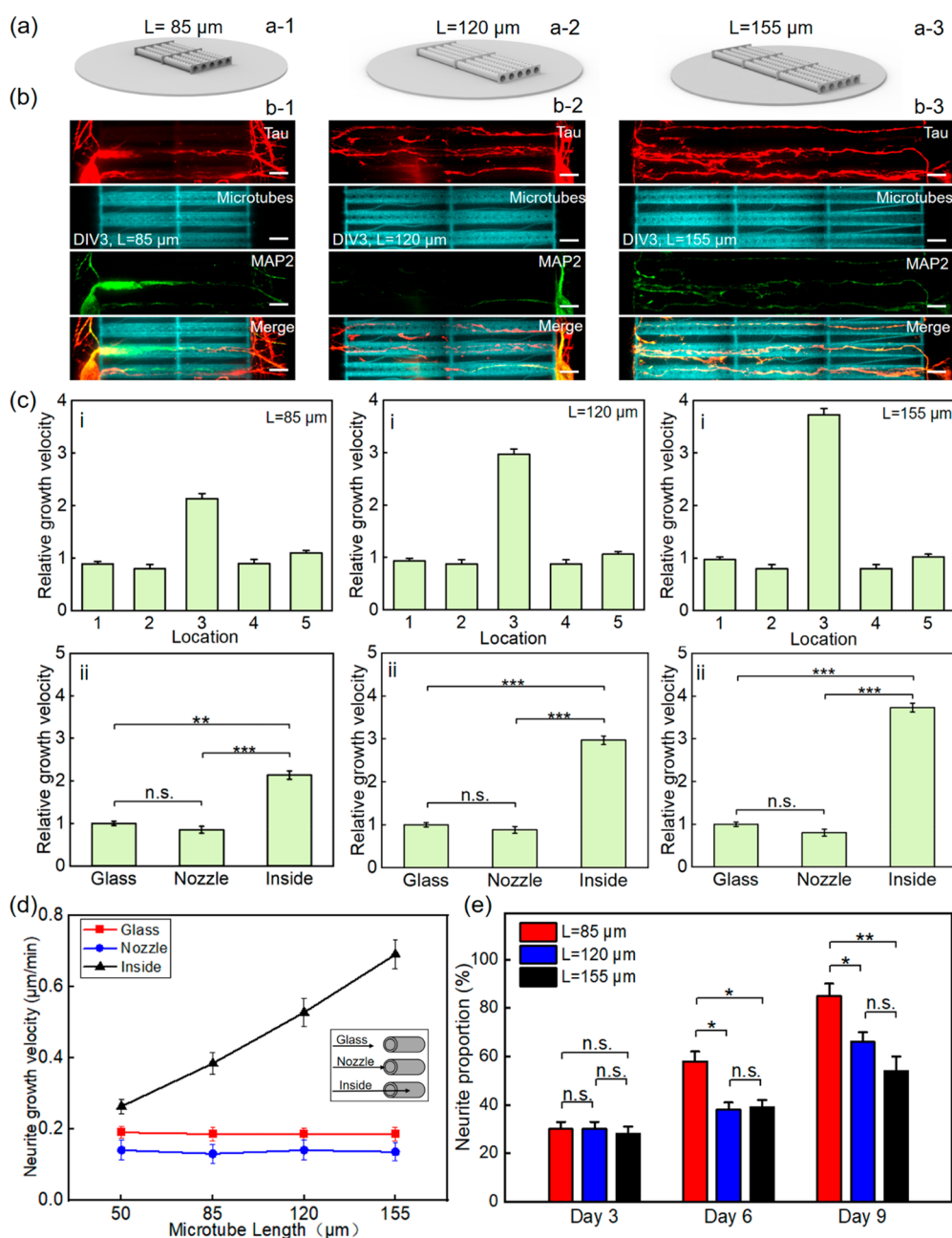
Figure 4. Accelerated growth of neurites by microtubes: effect of microtube length. (a) Schematic diagram of microtubes with lengths of 85 μm (a-1), 120 μm (a-2), and 155 μm (a-3). (b) Representative fluorescence microscopic images showing neurite growth on polylysine-coated microtubes with different lengths ((b-1): 85 μm; (b-2): 120 μm; (b-3): 155 μm) at 3 DIV (antibody labeled tau (red); microtubes (blue); antibody labeled MAP2 (green); merged panels combining three images, tau, microtubes, and MAP2). (c) (i) Relative growth velocity (μm/min) calculated from the living cell recording. (ii) The relative growth velocity is calculated at the glass, microtube nozzles, and inside microtubes. (d) The line chart shows the neurite growth velocity of microtubes with different lengths in glass, microtube nozzles, and inside microtubes. (e) The proportion of neurite growth in microtubes with different lengths at 3, 6, and 9 DIV. (n = 15 samples and three separate cultures each). The Origin software package was used for the statistical analysis, followed by one-way ANOVA (*$p < 0.05$, **$p < 0.01$, ***$p < 0.001$, n.s., no significance). Here, the microtubes have an inner diameter of 6 μm and a wall thickness of 1 μm. Scale = 10 μm.

conclusions because of the accelerated growth of neurites). Thinner walls easily cause the microtubes to break, whereas thicker walls are too stiff to affect the neuronal growth environments. Therefore, it is very important to choose microtubes with appropriate wall thickness. The microtubes with wall thicknesses of 0.5, 0.75, and 1 μm were designed and fabricated for studying neurite outgrowth (Figure 3a; when the wall thickness was less than 0.5 μm, the microtubes easily collapsed). In the microtube with a wall thickness of 0.5 μm,

the behaviors of the axonal growth cone (Figure S13, Video S6) are the same as those in the microtube with wall thicknesses of 0.75 and 1 μm (Video S7); again, inside the microtubes, the growth of neurites is accelerated (Figure 3b; the rates of the growth acceleration of neurites in the microtubes with 0.5, 0.75, and 1 μm were approximately 11.11, 10.75, and 9.77 μm/h^2, respectively). In contrast to the microtube with a wall thickness of 1 μm, the speed of neurite growth inside the microtube with a wall thickness of 0.5 or
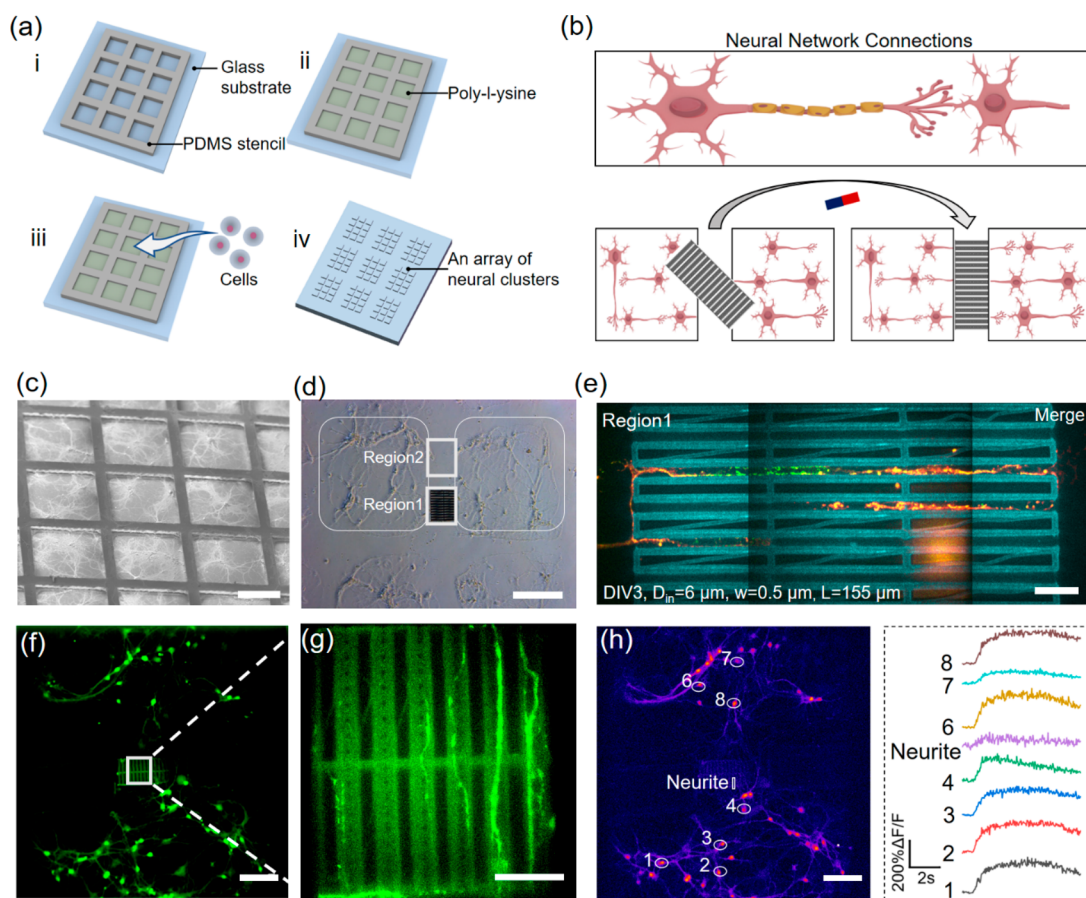
Figure 5. Magnetically manipulated microtubes for selective connection of neurons. (a) Fabrication process of an array of neural clusters on a glass substrate. (i) The PDMS stencil is placed on a glass substrate. (ii) Polylysine is coated for cell attachment. (iii) The primary hippocampal neurons are seeded on the glass substrate. (iv) The removal of the PDMS stencil from the glass substrate. (b) Schematic of the active neural network connections between two neural clusters using a magnetic microtube array. (c) An SEM image shows that primary hippocampal neurons are seeded on the glass substrate attached to a PDMS stencil at 3 DIV. (d) A magnetic microtube array is manipulated to connect two clusters of neurons. Region 1 is the microtube array ,and region 2 is the area without the microtube array. (e) Representative fluorescence microscopic image shows that neurites in microtubes grow and connect neural clusters at 6 DIV. Antibody labeled tau (red), microtubes (blue), antibody labeled MAP2 (green), and merged panels combining three images, tau, microtubes and MAP2. (f—h) Monitoring neuronal activity in networks by Ca^{2+} imaging on magnetic microtubes (11 DIV). (f) Fluo-8 labeled hippocampal neurons. (g) A magnified view of neurites within microtubes corresponds to the square of Figure 5f. (h) Pseudocolor MIP (maximum intensity projection) image of the fluorescence change ($\Delta F/F_{median}$) shows the fluorescence intensity change of hippocampal neurons during 10 s, and the bright color region represents the neuronal action potential that occurred in this period (left), Ca^{2+} imaging $\Delta F/F$ trace of eight positions (right). (c,d) Scale = 300 μm. (e) Scale = 15 μm. (f,h) Scale = 100 μm. (g) Scale = 20 μm.

0.75 μm (Figure 3c−e, Figure S14) is higher and reaches approximately 20 μm/h. Compared with the growth velocity of neurons on glass substrates, the fastest speed of neurites in microtubes with a wall thickness of 0.5 μm sometimes increased by ∼10-fold (Video S8).

Generally, the growth speed of neurites in the microtubes is significantly higher than that at the microtube inlets and outlets and on the glass substrates. In addition, the thinner the wall of the microtubes is, the faster the growth of neurites in the microtubes is (Figure 3c). Additionally, the proportion of neurites increased with culture time, but the increase in the thickness caused a decrease in the proportion (Figure S15), resulting from the increase in the pathfinding time of the growth cone (Figure 3f).

Accelerated growth of neurites by microtubes: effect of microtube length. Previously, Froeter et al.[19] showed that a self-rolled-up microtube with a length of 50 μm can increase the growth speed of neurites. Here, the lengths of the microtubes are appropriately increased to 85, 120, and 155 μm (Figure 4a; the connecting part in the middle of microtubes is to avoid the

adhesion of microtubes). Here, an interesting phenomenon is that even if the microtubes are very long, neural circuits can still be easily formed between neurons (Figure 4b). The results show that for the long microtubes, the speed of neurite growth in the microtubes is far larger than that at the nozzle or on glass (Figure 4c). Furthermore, the longer the microtube length is, the longer the acceleration time is (even for 155 μm microtubes, the scale is still very small, and we speculate that at the scale, the growth is still accelerating), and the faster the growth velocity of neurites in the microtubes is. In 85, 120, and 155 μm microtubes, the average growth velocities of neurites reached 23, 32, and 41 μm/h (Figure 4d; Videos S9, S10, and S11), respectively, and the rates of the growth acceleration were approximately 10.63, 11.34, and 11.04 μm/h^2, respectively (the results confirmed the speculation we mentioned above). We also summarize the relative speed of neurite growth within microtubes with different sizes at different locations (Figures S16−S18).

Generally, the speed of neurite growth is closely related to the diameter of axons and dendrites, the presence or absence

of myelin sheaths, temperature, etc.[32,33] Myelinated neurites grow faster than unmyelinated neurites. We think that the microfabricated porous microtubes act in part as a myelin sheath, contributing to the enhanced axon and dendrite guidance by radial constraint and promoting the accelerated growth of axons and dendrites. With increasing culture time, the number of neurites in the microtubes increased. However, after 9 DIV, the proportion of neurites in microtubes with a length of 155 μm was only 54% (Figure 4e). To explore this reason, we carefully observed the growth cones and found that the retraction of growth cones in pathfinding occurred, especially in long microtubes. Thus, we speculated that the neuron sensory process possibly works only within a certain length range because the rates of synthesis and transportation of certain proteins are limited for neurons themselves. Here, we also find an interesting phenomenon: when the growth cone senses an edge, it tends to continue its trajectory across the edge to sense the next cue (the microtube array) rather than align with the edge (Video S12). The possible mechanism for this phenomenon is that by some certain polarization markers, the growth cones of neurons are sensitive to topographic cues,[19,34] and then, the neurites are oriented.[35]

Magnetically manipulated microtubes for the selective connection of neurons. The selective connection of neurons ensures the expected directional conduction in a specific neural circuit, which is an indispensable process for the development of the nervous system. Here, we fabricate a magnetically actuated microtube array that also has the capability for the selective connection of neurons.

To confirm the ability of the magnetically actuated microtube array to selectively connect neurons, neural clusters are isolated, cultured, and attached at predetermined regions (Figure 5a; an array of 500 μm by 500 μm neural clusters with a gap of approximately 100 μm is patterned on a glass substrate), and then, the magnetic microtube array is manipulated between two adjacent regions with neural clusters by a permanent magnet (Figure 5b). Figures 5c and S19 show the neural clusters cultured in the polydimethylsiloxane (PDMS) stencil on the glass substrate and attached neural clusters on the glass substrate after removing the PDMS stencil. Then, the magnetic microtubes are moved to a designated region to selectively connect the left and right neural clusters (Figure 5d, Region 1). Since the microtubes are deposited with very thin layers of Ni and Ti, the neurites are immunostained and observed (Figure 5e). The neurites only appear in the magnetic microtubes rather than the regions in the absence of microtubes (Figure 5d, Region 2), indicating the morphological selective connection of neurons by the magnetic microtubes (Figure 5e). The patch clamp also confirms the connection of neurons through the microtubes (Figure S20).

To further confirm the successful functional connection of neurons, Ca^{2+} imaging was used to monitor neuron activity in adjacent neural cluster regions. Under the confocal microscope, neuron morphologies can be observed (Figure 5f,g). Here, by imaging the spontaneous Ca^{2+} activity of neurons at both ends of microtubes, we show synchronized firing between the neuron clusters (Figure 5h). However, there was no synchronous burst of activity between isolated neuron clusters without microtube connections (Figure S21). These findings demonstrate successful synaptic signaling between nerve clusters that are selectively connected by the magnetic microtubes we fabricate.

In this study, we propose porous microtubes for accelerating the growth of neurites and directing neuronal connections. The coaxial constraints of microtubes on axons or dendrites are very similar to myelin sheaths in the nervous system. Using one-step fs-DLW, we successfully fabricate microtubes with different inner diameters, wall thicknesses, and lengths. The microtube arrays provide extremely well-defined guidance and dramatically increased growth velocity for hippocampal neurons. Compared with glass substrates and other sizes of microtubes, microtubes with an inner diameter of 6 μm, a wall thickness of 1 μm, and a length of 155 μm show the fastest growth velocity in terms of accelerating the growth of neurites. Furthermore, we successfully achieved the *in vitro* selective/ directive connections of neural clusters using a magnetic microtube array. The microtubes proposed here may enable us to rapidly replicate complex biological neural networks, providing a powerful platform for the development of therapeutic interventions and the understanding of neural networks.

■ ASSOCIATED CONTENT

ⓈSupporting Information

The Supporting Information is available free of charge at https://pubs.acs.org/doi/10.1021/acs.nanolett.2c03232.

> Video S1. The magnetic microtubes passing through a designed "N" shaped pattern. Scale = 100 μm (MP4)
>
> Video S2. The magnetic microtubes passing through a designed "L" shaped pattern. Scale = 100 μm (MP4)
>
> Video S3. The magnetic microtubes passing through a designed square pattern. Scale = 100 μm (MP4)
>
> Video S4. Porous 3D microtubes with a wall thickness of 0.75 μm and an inner diameter of 6 μm guide neurite growth. Scale = 10 μm (MP4)
>
> Video S5. Porous 3D microtubes with a wall thickness of 0.5 μm and an inner diameter of 2 μm guide neurite growth. Scale = 10 μm (MP4)
>
> Video S6. Porous 3D microtubes with a wall thickness of 0.75 μm and an inner diameter of 6 μm guide neurite growth. Scale = 10 μm (MP4)
>
> Video S7. Porous 3D microtubes with a wall thickness of 1 μm and an inner diameter of 6 μm guide neurite growth. Scale = 10 μm (MP4)
>
> Video S8. Porous 3D microtubes with a wall thickness of 0.5 μm and an inner diameter of 6 μm guide neurite growth. Scale = 10 μm (MP4)
>
> Video S9. Porous 3D microtubes with a wall thickness of 1 μm, a length of 85 μm, and an inner diameter of 6 μm guide neurite growth. Scale = 15 μm (MP4)
>
> Video S10. Porous 3D microtubes with a wall thickness of 1 μm, a length of 120 μm, and an inner diameter of 6 μm guide neurite growth. Scale = 15 μm (MP4)
>
> Video S11. Porous 3D microtubes with a wall thickness of 1 μm, a length of 155 μm, and an inner diameter of 6 μm guide neurite growth. Scale = 20 μm (MP4)
>
> Video S12. Porous 3D two-stage microtubes with a wall thickness of 0.5 μm, a length of 85 μm, and an inner diameter of 6 μm guide neurite growth. Scale = 10 μm (MP4)
>
> Supporting Information for "Accelerating Neurite Growth and Directing Neuronal Connections Constrained by 3D Porous Microtubes" (PDF)

AUTHOR INFORMATION

Corresponding Authors

Jiawen Li − *Key Laboratory of Precision Scientific Instrumentation of Anhui Higher Education Institutes, CAS Key Laboratory of Mechanical Behavior and Design of Materials, Department of Precision Machinery and Precision Instrumentation, University of Science and Technology of China, Hefei, Anhui 230026, China;* ⊙ orcid.org/0000-0003-3950-6212; Email: jwl@ustc.edu.cn

Pakming Lau − *Institute of Artificial Intelligence, Hefei Comprehensive National Science Center, Hefei, Anhui 230026, China; CAS Key Laboratory of Brain Function and Disease, School of Life Sciences, Division of Life Sciences and Medicine, University of Science and Technology of China, Hefei, Anhui 230026, China;* Email: plau@ustc.edu.cn

Weiping Ding − *Department of Oncology, the First Affiliated Hospital of USTC, Division of Life Sciences and Medicine, University of Science and Technology of China, Hefei, Anhui 230001, China;* ⊙ orcid.org/0000-0002-3331-1011; Email: wpdings@ustc.edu.cn

Authors

Shengying Fan − *Department of Electronic Engineering and Information Science, University of Science and Technology of China, Hefei, Anhui 230026, China; Department of Oncology, the First Affiliated Hospital of USTC, Division of Life Sciences and Medicine, University of Science and Technology of China, Hefei, Anhui 230001, China*

Lei Qi − *Institute of Artificial Intelligence, Hefei Comprehensive National Science Center, Hefei, Anhui 230026, China*

Shunli Liu − *Key Laboratory of Precision Scientific Instrumentation of Anhui Higher Education Institutes, CAS Key Laboratory of Mechanical Behavior and Design of Materials, Department of Precision Machinery and Precision Instrumentation, University of Science and Technology of China, Hefei, Anhui 230026, China*

Rui Li − *Key Laboratory of Precision Scientific Instrumentation of Anhui Higher Education Institutes, CAS Key Laboratory of Mechanical Behavior and Design of Materials, Department of Precision Machinery and Precision Instrumentation, University of Science and Technology of China, Hefei, Anhui 230026, China*

Tongzhou Zhan − *Key Laboratory of Precision Scientific Instrumentation of Anhui Higher Education Institutes, CAS Key Laboratory of Mechanical Behavior and Design of Materials, Department of Precision Machinery and Precision Instrumentation, University of Science and Technology of China, Hefei, Anhui 230026, China*

Xiaowei Li − *CAS Key Laboratory of Brain Function and Disease, School of Life Sciences, Division of Life Sciences and Medicine, University of Science and Technology of China, Hefei, Anhui 230026, China*

Dong Wu − *Key Laboratory of Precision Scientific Instrumentation of Anhui Higher Education Institutes, CAS Key Laboratory of Mechanical Behavior and Design of Materials, Department of Precision Machinery and Precision Instrumentation, University of Science and Technology of China, Hefei, Anhui 230026, China;* ⊙ orcid.org/0000-0003-0623-1515

Bensheng Qiu − *Department of Electronic Engineering and Information Science, University of Science and Technology of China, Hefei, Anhui 230026, China;* ⊙ orcid.org/0000-0003-2987-7378

Guoqiang Bi − *CAS Key Laboratory of Brain Function and Disease, School of Life Sciences, Division of Life Sciences and Medicine, University of Science and Technology of China, Hefei, Anhui 230026, China*

Complete contact information is available at:
https://pubs.acs.org/10.1021/acs.nanolett.2c03232

Author Contributions

The manuscript was written through contributions of all authors. All authors have given approval to the final version of the manuscript. These authors contributed equally: Shengying Fan, Lei Qi.

Notes

The authors declare no competing financial interest.

REFERENCES

(1) Hua, J. Y.; Smith, S. J. Neural activity and the dynamics of central nervous system development. *Nature neuroscience* **2004**, *7* (4), 327−332.

(2) Silva, A. J.; Zhou, Y.; Rogerson, T.; Shobe, J.; Balaji, J. Molecular and cellular approaches to memory allocation in neural circuits. *Science* **2009**, *326* (5951), 391−395.

(3) Marom, S.; Shahaf, G. Development, learning and memory in large random networks of cortical neurons: lessons beyond anatomy. *Q. Rev. Biophys.* **2002**, *35* (1), 63−87.

(4) Lau, P.-M.; Bi, G.-Q. Synaptic mechanisms of persistent reverberatory activity in neuronal networks. *Proc. Natl. Acad. Sci. U. S. A.* **2005**, *102* (29), 10333−10338.

(5) Bradke, F.; Fawcett, J. W.; Spira, M. E. Assembly of a new growth cone after axotomy: the precursor to axon regeneration. *Nat. Rev. Neurosci.* **2012**, *13* (3), 183−193.

(6) Kam, L.; Shain, W.; Turner, J.; Bizios, R. Axonal outgrowth of hippocampal neurons on micro-scale networks of polylysine-conjugated laminin. *Biomaterials* **2001**, *22* (10), 1049−1054.

(7) Roth, S.; Bugnicourt, G.; Bisbal, M.; Gory Fauré, S.; Brocard, J.; Villard, C. Neuronal Architectures with Axon dendritic Polarity above Silicon Nanowires. *Small* **2012**, *8* (5), 671−675.

(8) Greene, A. C.; Washburn, C. M.; Bachand, G. D.; James, C. D. Combined chemical and topographical guidance cues for directing cytoarchitectural polarization in primary neurons. *Biomaterials* **2011**, *32* (34), 8860−8869.

(9) Yoshida, S.; Teshima, T.; Kuribayashi Shigetomi, K.; Takeuchi, S. Mobile microplates for morphological control and assembly of individual neural cells. *Adv. Healthcare Mater.* **2016**, *5* (4), 415−420.

(10) Kim, S.; Im, W.-S.; Kang, L.; Lee, S.-T.; Chu, K.; Kim, B. I. The application of magnets directs the orientation of neurite outgrowth in cultured human neuronal cells. *Journal of neuroscience methods* **2008**, *174* (1), 91−96.

(11) Kim, E.; Jeon, S.; An, H.-K.; Kianpour, M.; Yu, S.-W.; Kim, J.-y.; Rah, J.-C.; Choi, H. A magnetically actuated microrobot for targeted neural cell delivery and selective connection of neural networks. *Science advances* **2020**, *6* (39), eabb5696.

(12) Sherman, D. L.; Brophy, P. J. Mechanisms of axon ensheathment and myelin growth. *Nat. Rev. Neurosci.* **2005**, *6* (9), 683−690.

(13) Park, J.; Jeon, J.; Kim, B.; Lee, M. S.; Park, S.; Lim, J.; Yi, J.; Lee, H.; Yang, H. S.; Lee, J. Y. Electrically conductive hydrogel nerve guidance conduits for peripheral nerve regeneration. *Adv. Funct. Mater.* **2020**, *30* (39), 2003759.

(14) Huang, Q.; Cai, Y.; Yang, X.; Li, W.; Pu, H.; Liu, Z.; Liu, H.; Tamtaji, M.; Xu, F.; Sheng, L.; et al. Graphene foam/hydrogel scaffolds for regeneration of peripheral nerve using ADSCs in a diabetic mouse model. *Nano Research* **2022**, *15* (4), 3434−3445.

(15) Qian, Y.; Zhao, X.; Han, Q.; Chen, W.; Li, H.; Yuan, W. An integrated multi-layer 3D-fabrication of PDA/RGD coated graphene loaded PCL nanoscaffold for peripheral nerve restoration. *Nat. Commun.* **2018**, *9* (1), 323.

(16) Tao, J.; Zhang, J.; Du, T.; Xu, X.; Deng, X.; Chen, S.; Liu, J.; Chen, Y.; Liu, X.; Xiong, M.; et al. Rapid 3D printing of functional nanoparticle-enhanced conduits for effective nerve repair. *Acta biomaterialia* **2019**, *90*, 49−59.

(17) Cheng, Y.; Xu, Y.; Qian, Y.; Chen, X.; Ouyang, Y.; Yuan, W. E. 3D structured self-powered PVDF/PCL scaffolds for peripheral nerve regeneration. *Nano Energy* **2020**, *69*, 104411.

(18) Liu, K.; Yan, L.; Li, R.; Song, Z.; Ding, J.; Liu, B.; Chen, X. 3D Printed Personalized Nerve Guide Conduits for Precision Repair of Peripheral Nerve Defects. *Advanced Science* **2022**, *9* (12), 2103875.

(19) Froeter, P.; Huang, Y.; Cangellaris, O. V.; Huang, W.; Dent, E. W.; Gillette, M. U.; Williams, J. C.; Li, X. Toward intelligent synthetic neural circuits: Directing and accelerating neuron cell growth by self-rolled-up silicon nitride microtube array. *ACS Nano* **2014**, *8* (11), 11108−11117.

(20) Cangellaris, O. V.; Corbin, E. A.; Froeter, P.; Michaels, J. A.; Li, X.; Gillette, M. U. Aligning synthetic hippocampal neural circuits via self-rolled-up silicon nitride microtube arrays. *ACS Appl. Mater. Interfaces* **2018**, *10* (42), 35705−35714.

(21) Greiner, A. M.; Richter, B.; Bastmeyer, M. Micro engineered 3D scaffolds for cell culture studies. *Macromol. Biosci.* **2012**, *12* (10), 1301−1314.

(22) Larramendy, F.; Yoshida, S.; Maier, D.; Fekete, Z.; Takeuchi, S.; Paul, O. 3D arrays of microcages by two-photon lithography for spatial organization of living cells. *Lab Chip* **2019**, *19* (5), 875−884.

(23) Murphy, A. R.; Haynes, J. M.; Laslett, A. L.; Cameron, N. R.; O'Brien, C. M. Three-dimensional differentiation of human pluripotent stem cell-derived neural precursor cells using tailored porous polymer scaffolds. *Acta Biomater.* **2020**, *101*, 102−116.

(24) Wei, Z.; Sun, T.; Shimoda, S.; Chen, Z.; Chen, X.; Wang, H.; Huang, Q.; Fukuda, T.; Shi, Q. Bio-inspired engineering of a perfusion culture platform for guided three-dimensional nerve cell growth and differentiation. *Lab Chip* **2022**, *22* (5), 1006−1017.

(25) Tonazzini, I.; Masciullo, C.; Savi, E.; Sonato, A.; Romanato, F.; Cecchini, M. Neuronal contact guidance and YAP signaling on ultra-small nanogratings. *Sci. Rep.* **2020**, *10* (1), 3742.

(26) Grove, M.; Brophy, P. J. FAK is required for Schwann cell spreading on immature basal lamina to coordinate the radial sorting of peripheral axons with myelination. *J. Neurosci.* **2014**, *34* (40), 13422−13434.

(27) Fukuda, K.; Knight, J. D.; Piszczek, G.; Kothary, R.; Qin, J. Biochemical, proteomic, structural, and thermodynamic character-izations of integrin-linked kinase (ILK): cross-validation of the pseudokinase. *J. Biol. Chem.* **2011**, *286* (24), 21886−21895.

(28) Xue, W.; Shi, W.; Kong, Y.; Kuss, M.; Duan, B. Anisotropic scaffolds for peripheral nerve and spinal cord regeneration. *Bioactive materials* **2021**, *6* (11), 4141−4160.

(29) Dent, E. W.; Gertler, F. B. Cytoskeletal dynamics and transport in growth cone motility and axon guidance. *Neuron.* **2003**, *40* (2), 209−227.

(30) Craig, E. M.; Van Goor, D.; Forscher, P.; Mogilner, A. Membrane tension, myosin force, and actin turnover maintain actin treadmill in the nerve growth cone. *Biophysical journal* **2012**, *102* (7), 1503−1513.

(31) Basso, J. M. V.; Yurchenko, I.; Wiens, M. R.; Staii, C. Neuron dynamics on directional surfaces. *Soft Matter.* **2019**, *15* (48), 9931−9941.

(32) Vensi Basso, J. M.; Yurchenko, I.; Simon, M.; Rizzo, D. J.; Staii, C. Role of geometrical cues in neuronal growth. *Phys. Rev. E* **2019**, *99* (2), 022408.

(33) Cohen, C. C.; Popovic, M. A.; Klooster, J.; Weil, M.-T.; Möbius, W.; Nave, K.-A.; Kole, M. H. Saltatory conduction along myelinated axons involves a periaxonal nanocircuit. *Cell.* **2020**, *180* (2), 311−322.e15.

(34) Szabó, Á.; Liliom, H.; Fekete, Z.; Schlett, K.; Pongrácz, A. SU-8 microstructures alter the attachment and growth of glial cells in vitro. *Materials Today Communications* **2021**, *27*, 102336.

(35) Micholt, L.; Gartner, A.; Prodanov, D.; Braeken, D.; Dotti, C. G.; Bartic, C. Substrate topography determines neuronal polarization and growth in vitro. *PLoS One* **2013**, *8* (6), e66170.

▣ Recommended by ACS